Validation of Volume-Preserving Non-rigid Registration: Application to Contrast-Enhanced MR-Mammography

C. Tanner[1], J.A. Schnabel[1], A. Degenhard[2], A.D. Castellano-Smith[1], C. Hayes[2], M.O. Leach[2], D.R. Hose[3], D.L.G. Hill[1], and D.J. Hawkes[1]

[1] Div. of Radiological Sciences & Medical Engineering, King's College London, UK
[2] Section of MR, Inst. of Cancer Research & Royal Marsden NHS Trust, Sutton, UK
[3] Dept. of Medical Physics and Clinical Engineering, University of Sheffield, UK
christine.tanner@kcl.ac.uk

Abstract. In this paper, we present a validation study for volume preserving non-rigid registration of 3D contrast-enhanced magnetic resonance mammograms. This study allows for the first time to assess the effectiveness of a volume preserving constraint to improve registration accuracy in this context. The validation is based on the simulation of physically plausible breast deformations with biomechanical breast models (BBMs) employing finite element methods. We constructed BBMs for four patients with four different deformation scenarios each. These deformations were applied to the post-contrast image to simulate patient motion occurring between pre- and post-contrast image acquisition. The original pre-contrast images were registered to the corresponding BBM-deformed post-contrast images. We assessed the accuracy of two optimisation schemes of a non-rigid registration algorithm. The first solely aims to improve the similarity of the images while the second includes the minimisation of volume changes as another objective. We observed reductions in residual registration error at every resolution when constraining the registration to preserve volume. Within the contrast enhancing lesion, the best results were obtained with a control point spacing of 20mm, resulting in target registration errors below 0.5mm on average. This study forms an important milestone in making the non-rigid registration framework applicable for clinical routine use.

1 Introduction

Contrast-enhanced magnetic resonance (CE MR) mammography is based on obtaining MR images before and after the injection of contrast agent into the bloodstream. Breast cancer malignancies can be detected in-vivo by their increased vascularity, increased vascular permeability and/or increased interstitial pressure [1, 2], causing a rapid rise in the intensity of CE MR-mammograms. However, a considerable proportion of benign lesions also enhance. The rate and amount of the enhancement as well as the characteristics of the intensity changes after the peak enhancement need to be taken into account if specificity is to be improved [3].

The detailed quantitative analysis of the intensity changes over time relies on the accurate alignment of all images. Patient movement will introduce correspondence errors that may invalidate such an analysis. Previously, an algorithm has been devised for

T. Dohi and R. Kikinis (Eds.): MICCAI 2002, LNCS 2488, pp. 307–314, 2002.

the non-rigid registration of images [4] and applied to CE MR-mammograms. It was shown that this registration method significantly improved the quality of the pre- and post-contrast image difference [5].

Generally, non-rigid registration algorithms can change the volume of structures. This is for example necessary for inter-subject registration. Volume changes are, however, physically implausible during a CE MR-mammography acquisition since no external forces are applied to the breast and the gap between image acquisitions is short. In [6] we evaluated the volume change associated with non-rigid registration of 15 contrast enhancing breast lesions and found volume shrinkage and expansion of up to 20%. Previously, volume changes were reduced by the introduction of a volume preserving regularization term to the registration's optimisation scheme [7–9]. The question remains, however, how to measure the residual registration error since no ground truth exists.

In [10] we have proposed validation of non-rigid registration algorithms on the basis of applying it to misaligned images, generated from plausible deformations simulated by biomechanical models. This generic method has the advantage of providing a displacement vector at every position within the organ. We have employed this method for validating two non-rigid registration algorithms [4, 11] based on single and multi-level free-form deformations (FFDs) using B-splines and normalised mutual information [12] and found an improved accuracy for the multi-level FFD approach. In this validation study we will for the first time assess the influence of volume preserving constraints on the target registration error for a multi-resolution FFD non-rigid registration for the application of CE MR-mammography.

2 Materials

We selected from a large CE-MR mammography database four cases where almost no motion between image acquisitions was visible. The images have been acquired with a 3D gradient echo sequence on a Philips (case 1-3) or a Siemens (case 4) 1.5T MR system with TR=12ms, TE=5ms, flip angle=35^o and a field of view of 350mm (case 1-3) or 340mm (case 4). The voxel dimensions are 1.37x1.37x4.2mm^3 (case 1-2), 1.48x1.48x4.2mm^3 (case 3) and 1.33x1.33x2.5mm^3 (case 4). The slice orientation is axial (case 1-3) or coronal (case 4). Example slices of the difference of the original images are shown in Fig. 1a, where case 4 was reformatted to have an axial slice direction for better visual comparison.

3 Methods

3.1 Registration

In this study the non-rigid registration is based on the multi-resolution FFD approach based on accurate B-spline subdivision as described in [4]. In comparison to the multi-level FFD approach [11], this has the advantage that the analytical Jacobian of the transformation can be effectively determined at each resolution. Firstly, global motion is corrected by using a rigid transformation. Local motion is then modelled by FFDs

based on B-splines where the object is deformed by manipulating an underlying mesh of control points. Starting from a coarser mesh to account for the larger deformations, the mesh is subdivided at each resolution to give the FFDs more local flexibility. At any stage, the transformation $\mathbf{T}$ between the images A and B can be described as the sum of the global 3D rigid transformation $\mathbf{T}_g$ and the local FFD transformation $\mathbf{T}_l$, i.e. $\mathbf{T}(\mathbf{x}) = \mathbf{T}_g(\mathbf{x}) + \mathbf{T}_l(\mathbf{x})$. This transformation maps the position $\mathbf{x} = (x_1\ x_2\ x_3)^T$ in A to the corresponding position $T(\mathbf{x})$ in B.

FFD transformation. Let $\Omega = \{\mathbf{x} \,|\, 0 \leq x_i < X_i,\ i \in \{1,2,3\}\}$ be the domain of the image volume and let $\Psi = \{\psi_{j_1,j_2,j_3} \,|\, j_i \in \{0,1,\ldots,N_i-1\},\ i \in \{1,2,3\}\}$ be the mesh of control points with displacements $\phi^{(i)}_{j_1,j_2,j_3}$ and spacing $\delta_i = \frac{X_i}{N_i-1}$ for $i \in \{1,2,3\}$. $\mathbf{T}_l(\mathbf{x}) = (T_l^{(1)}(\mathbf{x})\ T_l^{(2)}(\mathbf{x})\ T_l^{(3)}(\mathbf{x}))^T$ can then be written as:

$$T_l^{(i)}(\mathbf{x}) = \sum_{m_1=0}^{3}\sum_{m_2=0}^{3}\sum_{m_3=0}^{3}\prod_{k=1}^{3} B_{m_k}(u_k)\phi^{(i)}_{j_1+m_1,j_2+m_2,j_3+m_3} \quad i \in \{1,2,3\} \tag{1}$$

where $j_i = \lfloor \frac{x_i}{\delta_i} \rfloor - 1$, $u_i = \frac{x_i}{\delta_i} - \lfloor \frac{x_i}{\delta_i} \rfloor$ for $i \in \{1,2,3\}$ and B_m is the m-th basis function of the B-spline defined by:

$B_0(u) = (1-u)^3/6$ $\qquad$ $B_2(u) = (-3u^3 + 3u^2 + 3u + 1)/6$

$B_1(u) = (3u^3 - 6u^2 + 4)/6$ $\qquad$ $B_3(u) = u^3/6$

Volume Preserving Regularization Term. In this validation we apply the volume preserving regularization term suggested by Rohlfing et al. [9]. The local volume change at position $\mathbf{x}$ after applying transformation $\mathbf{T}$ can be calculated by the determinant of the Jacobian:

$$J_{\mathbf{T}}(\mathbf{x}) = \det \begin{pmatrix} \frac{\partial}{\partial x_1}T_l^{(1)}(\mathbf{x}) & \frac{\partial}{\partial x_2}T_l^{(1)}(\mathbf{x}) & \frac{\partial}{\partial x_3}T_l^{(1)}(\mathbf{x}) \\ \frac{\partial}{\partial x_1}T_l^{(2)}(\mathbf{x}) & \frac{\partial}{\partial x_2}T_l^{(2)}(\mathbf{x}) & \frac{\partial}{\partial x_3}T_l^{(2)}(\mathbf{x}) \\ \frac{\partial}{\partial x_1}T_l^{(3)}(\mathbf{x}) & \frac{\partial}{\partial x_2}T_l^{(3)}(\mathbf{x}) & \frac{\partial}{\partial x_3}T_l^{(3)}(\mathbf{x}) \end{pmatrix} \tag{2}$$

where

$$\frac{\partial T_l^{(i)}(\mathbf{x})}{\partial x_n} = \frac{1}{\delta_n}\sum_{m_1=0}^{3}\sum_{m_2=0}^{3}\sum_{m_3=0}^{3}\frac{dB_{m_n}(u_n)}{du_n}\prod_{k\in\{1,2,3\}\cap n} B_{m_k}(u_k)\phi^{(i)}_{j_1+m_1,j_2+m_2,j_3+m_3}. \tag{3}$$

can be computed analytically. The regularization term for volume preservation from [9] is given by the mean absolute logarithm of the Jacobian at the control point positions:

$$C_{jacobian}(\mathbf{T}) = \frac{1}{N_1N_2N_3}\sum_{j_1=0}^{N_1-1}\sum_{j_2=0}^{N_2-1}\sum_{j_3=0}^{N_3-1} |\ln(J_{\mathbf{T}}(j_1\delta_1, j_2\delta_2, j_3\delta_3))|. \tag{4}$$

Volume shrinkage and expansion are equally penalised by (4). Transformation $\mathbf{T}$ is then found by minimising the cost function [9]:

$$C(\mathbf{T}) = -(1-\mu)C_{similarity}(A, \mathbf{T}(B)) + \mu C_{jacobian}(\mathbf{T}) \tag{5}$$

where μ is the weight of the volume preserving regularization term, that is balancing the two objectives of the cost function. Normalised mutual information (NMI) was used as the image similarity measure $C_{similarity}$.

3.2 Validation

The validation is based on the simulation of plausible breast deformation using biomechanical breast models based on finite element methods [10].

Biomechanical Breast Models. Four pre- and post-contrast image sets, which showed almost no motion, were selected from a large patient data base. The images were segmented into fat, glandular tissue and enhancing lesion. The outside surface of the fat and the enhancing lesion were then triangulated via vtk [13] and meshed into 10-noded tetrahedral elements with the ANSYS FEM package [14]. Elements within glandular tissue were assigned to have glandular material properties. All tissues were modelled as linear, isotropic and homogeneous. Elastic values (Young's modulus) of 1kPa, 1.5kPa, 3.6kPa were assigned to fat, glandular tissue and enhancing lesion, respectively, in accordance with [15]. Note that only the relative relationship of the Young's moduli are important since displacements rather than forces are applied. This model is therefore also very close to the values in [16] for 5% precompression. A Poisson's ratio of 0.495 was chosen to enforce incompressibility of the tissue. The average performance of this model is statistically (paired t-test) not significantly different at the 5% level to the best models from [17].

Simulation. Four different deformations were generated. 'Regional displacement' simulated a uniform displacement on one side of the breast, 'point puncture' imitated a deformation during biopsy, 'one-sided contact' simulated a deformation of the breast when pushed against the breast coil and 'two-sided contact' imitated the gentle fixation of the breast between two plates. All displacements were of maximal 10mm magnitude, which corresponds to the maximum offset observed during a normal CE MR-mammography session. For these boundary conditions, the BBMs were solved using ANSYS [14]. A continuous displacement field within the FEM mesh was produced by quadratic shape interpolation of the 10-noded tetrahedral elements. This field was applied to the post-contrast image to simulate deformations between pre- and post-contrast images. Locations outside the FEM-mesh had to be masked out for any further processing since no deformation information is available at these locations. We registered the pre-contrast images to the BBM-deformed post-contrast images to avoid any further interpolation of the latter.

Quantification. The accuracy of the registration can be quantified with respect to the gold standard displacements at each voxel position. The degree of alignment between two corresponding points after registration is described by the target registration error (TRE) [18]. Traditionally, TRE is calculated at anatomical landmarks. In the case of BBM-simulated deformations the correspondence is known at all position within the FEM mesh. We therefore calculate a more evenly distributed error by computing TRE at all voxel positions $\mathbf{x}$ within the FEM mesh:

$$TRE(\mathbf{x}) = ||\mathbf{T}_{2F} \circ \mathbf{T}_{F1}(\mathbf{x}) - \mathbf{x}|| \tag{6}$$

where $\mathbf{T}_{F1}$ is the FEM-transformation mapping any voxel position in the post-contrast image I_1 into the BBM-deformed post-contrast image I_F. Transformation $\mathbf{T}_{2F}$ is obtained from the registration of the pre-contrast image I_2 to I_F. Equation (6) assumes that no motion has occurred between I_2 and I_1. We can try to estimate how much motion has occurred from a registration of I_2 to I_1 yielding transformation $\mathbf{T}_{12}(\mathbf{x})$ which

in the ideal case is the identity transformation. This estimate can then be used to balance the TRE computation, providing a measure which we will call consistency registration error (CRE) [12]

$$CRE(\mathbf{x}) = ||\mathbf{T}_{12} \circ \mathbf{T}_{2F} \circ \mathbf{T}_{F1}(\mathbf{x}) - \mathbf{x}||. \quad (7)$$

4 Results

In this study, we investigated the registration performance of an unconstrained and a volume-preserving non-rigid registration scheme. All images were registered in a multi-resolution strategy, where an initial rigid registration was followed by non-rigid registrations of FFD resolutions of 20mm, 10mm and 5mm (see 3.1). The registration performance was assessed by calculating the target registration error (TRE) and consistency registration error (CRE) with respect to the simulated gold standard (see 3.2).

Regularization weight. A reasonable weight (μ_r) between image similarity and volume preservation was determined by calculating the volume change and the TRE for eight different values of μ within the range of 0.05 to 0.95 for two cases. In contrast to [9] we observed that a weight of 0.05 did not preserve volume. Mean volume shrinkage in these two cases was 13.2% without volume preservation and 13.0% with volume preservation. We chose μ_r=0.8, which reduced the shrinkage to 3.2% and provided the minimal median TRE over the whole breast tissue.

Validation. We conducted registrations of four patient cases and four BBM simulations each, for the volume preserving (μ=μ_r) and the unconstrained registration scheme (μ=0). Fig. 1b shows examples of motion artifacts introduced by the BBM simulated deformations. These artifacts are greatly reduced after unconstrained multi-resolution registration (Fig. 1d). Visually similar results are achieved by the volume preserving non-rigid registration (Fig. 1f). Local registration failures at highly deformed regions can be observed for the 20mm FFD registrations (Fig. 1c,e).

The volume changes before and after registration were evaluated over the whole breast tissue and for the enhancing lesion region (Table 1). The BBM simulation introduced absolute volume changes below 0.6%. Within the lesion, the maximum absolute volume change increased to 17.6% for the unconstrained registration, while for the volume preserving scheme it only increased to 5.1%.

The volume preserving non-rigid registration, produced at every FFD resolution, lower target registration errors when compared with the unconstrained method (Fig. 2a,b). Registrations with finer control point spacing compensated better for severe local deformations. However, within the region of the enhancing lesion, the best results were obtained with a control point spacing of 20mm. The consistency registration errors followed a similar trend (Fig. 2c,d). The 20mm FFD registration results were obtained on average within 2.2 and 1.7 hours for the unconstrained and the volume preserving scheme, respectively, on a 1.8 GHz Athon processor with 1GByte 1.33 MHz SD RAM memory. The full multi-resolution results (20mm+10mm+5mm) of the unconstrained and the volume preserving registration were available after 5.1 and 5.4 hours, respectively.

5 Discussion

We have presented a validation of an unconstrained and a volume preserving non-rigid registration scheme on the example of CE MR-mammography. The validation was based on simulating biomechanical plausible breast deformations as a gold standard.

We found that the volume preserving non-rigid registration was more accurate than the unconstrained method. Severe local deformations were better compensated by finer control point spacing. However, the contrast enhancing lesions were more accurately aligned at a control point spacing of 20mm.

This validation study has measured for the first time the target registration error of a volume preserving non-rigid registration. Our application is the alignment of dynamically acquired volumes in CE MR-mammograms. This is an important step towards making the registration techniques applicable for clinical routine use.

6 Acknowledgements

CT, AD and ADCS acknowledge funding from EPSRC (MIAS-IRC, GR/M52779, GR/M52762, GR/M47294). JAS is supported by Philips Medical Systems, EasyVision Advanced Development. The authors wish to thank Torsten Rohlfing for valuable discussions. The image data were provided by Guy's and St.Thomas' Hospitals (case 1-3) and by the UK MR breast screening study (MARIBS)
http://www.icr.ac.uk/cmagres/maribs/maribs.html (case 4).

References

1. C. H. Blood and B. R. Zetter, "Tumor Interactions with the Vasculature: Angiogensis and Tumor Metastasis," *Biochimica et Biophysica Acta*, vol. 1032, pp. 89–118, 1990.
2. P. W. Vaupel, *Blood Flow, Oxygenation, Tissue pH Distribution, and Bioenergetic Status of Tumors*. Berlin, Germany: Ernst Schering Research Foundation, 1st ed., 1994.
3. M. D. Schnall and D. M. Ikeda, "Lesion Diagnosis Working Group Report," *Journal of Magnetic Resonance Imaging*, vol. 10, pp. 982–990, 1999.
4. D. Rueckert, L. I. Sonoda, C. Hayes, D. L. Hill, M. O. Leach, and D. J. Hawkes, "Non-rigid Registration using Free-Form Deformations: Application to Breast MR Images," *IEEE Transactions on Medical Imaging*, vol. 7, pp. 1–10, August 1999.
5. E. R. E. Denton, L. I. Sonoda, D. Rueckert, S. C. Rankin, C. Hayes, M. O. Leach, and D. J. Hawkes, "Comparison and Evaluation of Rigid, Affine, and Nonrigid Registration of Breast MR Images," *Journal of Computer Assisted Tomography*, vol. 5, pp. 800–805, May 1999.
6. C. Tanner, J. A. Schnabel, D. Chung, M. J. Clarkson, D. Rueckert, D. L. G. Hill, and D. J. Hawkes, "Volume and Shape Preservation of Enhancing Lesions when Applying Non-rigid Registration to a Time Series of Contrast Enhanced MR Breast Images," in *Medical Image Computing and Computer-Assisted Intervention, Pittsburgh, USA*, pp. 327–337, 2000.
7. D. Terzopoulos and K. Waters, "Analysis and Synthesis of Facial Image Sequences using Physical and Anatomical Models," *IEEE Transactions on Pattern Analysis and Machine Intelligence*, vol. 15, pp. 569–579, 1993.
8. P. J. Edwards, D. L. G. Hill, J. A. Little, and D. J. Hawkes, "A Three-Component Deformation Model for Image-Guided Surgery," *Medical Image Analysis*, vol. 2, pp. 355–367, 1998.

9. T. Rohlfing and C. R. Maurer, "Intensity-Based Non-rigid Registration Using Adaptive Multilevel Free-Form Deformation with an Incompressibility Constraint," in *Medical Image Computing and Computer-Assisted Intervention, Utrecht, Netherlands*, pp. 111–119, 2001.
10. J. A. Schnabel, C. Tanner, A. D. Castellano-Smith, M. O. Leach, C. Hayes, A. Degenhard, R. Hose, D. L. G. Hill, and D. J. Hawkes, "Validation of Non-Rigid Registration using Finite Element Methods," in *Information Processing in Medical Imaging, Davis, CA, USA*, pp. 344–357, 2001.
11. J. A. Schnabel, D. Rueckert, M. Quist, J. M. Blackall, A. Castellano-Smith, T. Hartkens, G. P. Penney, W. A. Hall, C. L. Truwit, F. A. Gerritsen, D. L. G. Hill, and D. J. Hawkes, "A Generic Framework for Non-Rigid Registration based on Non-Uniform Multi-Level Free-Form Deformations," in *Medical Image Computing and Computer-Assisted Intervention, Utrecht, Netherlands*, pp. 573–581, 2001.
12. J. A. Schnabel, C. Tanner, A. D. Castellano-Smith, A. Degenhard, C. Hayes, M. O. Leach, D. R. Hose, and D. J. H. D. L. G. Hill, "Finite element based validation of non-rigid registration using single- and multi-level free-form deformations: Application to contrast-enhanced MR mammography," in *Proceedings SPIE Medical Imaging 2002, Image Processing, San Diego, CA*, pp. 550–581, 2002.
13. W. Schroeder, K. Martin, and B. Lorensen, *The Visualization Toolkit*. New Jersey, USA: Prentice Hall PTR, 2nd ed., 1998.
14. ANSYS. http://www.ansys.com.
15. A. Sarvazyan, D. Goukassian, E. Maevsky, and G. Oranskaja, "Elastic Imaging as a new Modality of Medical Imaging for Cancer Detection," in *Proceedings of the International Workshop on Interaction of Ultrasound with Biological Media, Valenciennes, France*, pp. 69–81, 1994.
16. T. A. Krouskop, T. M. Wheeler, F. Kallel, B. S. Garra, and T. Hall, "Elastic Moduli of Breast and Prostate Tissues Under Compression," *Ultrasonic Imaging*, vol. 20, pp. 260–274, 1998.
17. C. Tanner, A. Degenhard, J. A. Schnabel, A. Castellano-Smith, C. Hayes, L. I. Sonoda, M. O. Leach, D. R. Hose, D. L. G. Hill, and D. J. Hawkes, "A Comparison of Biomechanical Breast Models: A Case Study," in *Proceedings SPIE Medical Imaging 2002, Image Processing, San Diego, CA*, pp. 1807–1818, 2002.
18. J. M. Fitzpatrick, "Detecting failure, assessing success," in Hajnal *et al.* [19], ch. I-6, pp. 117–139.
19. J. V. Hajnal, D. L. G. Hill and D. J. Hawkes, eds., *Medical Image Registration*. CRC Press, 2001.

Volume change in %	whole breast tissue				enhancing lesion			
	mean	std	min	max	mean	std	min	max
BBM simulation	-0.10	0.13	-0.33	0.12	0.12	0.18	-0.03	0.57
20mm FFD, μ=0	-0.53	0.71	-1.93	0.77	-2.04	5.03	-17.64	2.53
10mm FFD, μ=0	-0.55	0.71	-1.95	0.76	-0.78	5.32	-13.53	5.95
5mm FFD, μ=0	-0.55	0.69	-1.93	0.77	-0.71	5.84	-15.50	6.85
20mm FFD, μ=0.8	-0.16	0.22	-0.75	0.08	0.08	0.90	-1.63	2.09
10mm FFD, μ=0.8	-0.17	0.26	-0.70	0.16	-0.38	1.47	-5.07	1.56
5mm FFD, μ=0.8	-0.18	0.31	-0.79	0.24	-0.16	1.05	-2.72	1.39

Table 1. Mean, standard deviation, minimal and maximal volume change of four patient cases and four BBM deformations each. Volume changes are evaluated over whole breast tissue (left) and over enhancing lesion (right) after BBM simulation and after multi-resolution FFD registration.

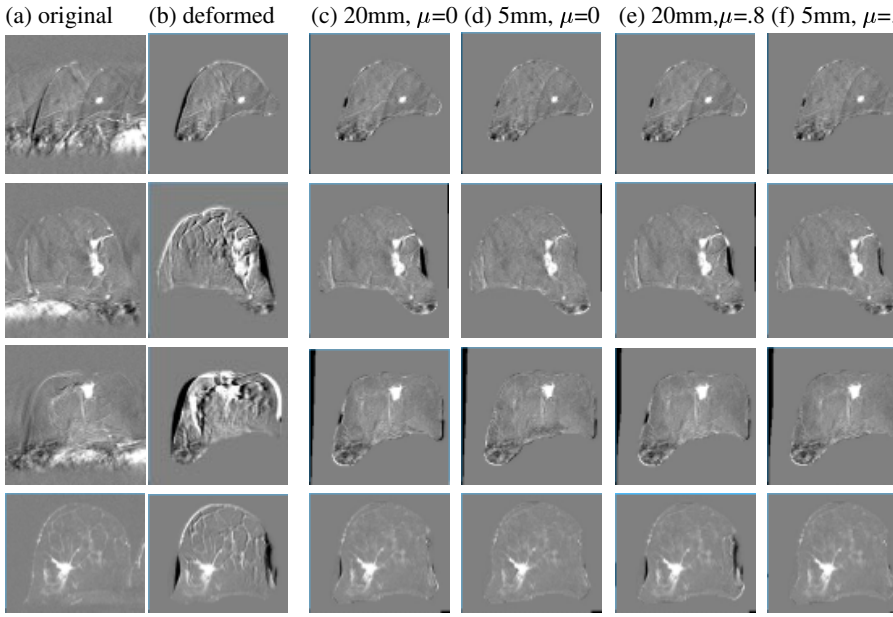

Fig. 1. Example slices for cases 1-4 (top to bottom) showing difference (a) of pre- and post-contrast images; (b) after deformation simulation; (c) after rigid + 20mm FFD registration without volume preveration constraint (μ=0); (d) after rigid + 20mm + 10mm + 5mm FFD registration with μ=0; (e) after rigid + 20mm FFD registration with μ=0.8; (f) after rigid + 20mm + 10mm + 5mm FFD registration with μ=0.8.

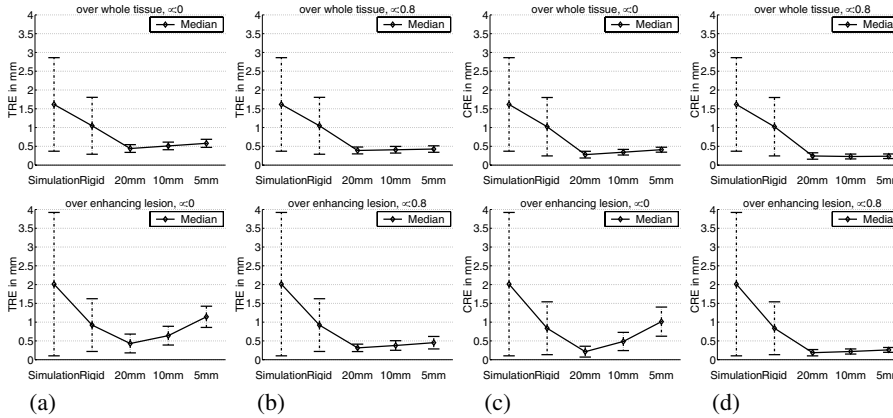

Fig. 2. Target registration error (TRE) for multi-resolution FFD registration (a) without volume preservation constraint (μ=0) and (b) for μ=0.8. Consistency registration error (CRE) for (c) μ=0 and (d) for μ=0.8. Top: Results evaluated over the whole breast tissue. Bottom: Results evaluated only over the region of the enhancing lesion. Error bars show the standard deviation from the mean over patients and simulations.